CHAPTER 61

ADJUSTMENT AND VERIFICATION OF THE RANDDELTA II MODEL

A. Langerak,[1] M. A. M. de Ras,[2] and J. J. Leendertse[3]

I. INTRODUCTION

In the mid-1950s the Netherlands government embarked on a massive construction program, called the Delta Plan. Its purpose was to enhance protection from floods caused by the North Sea in the estuaries of the Rhine, Meuse and Scheldt. According to the plan, all connections to the sea were to be closed by dams, except the New Waterway to Rotterdam and the Western Scheldt. In 1974 all dams and dikes were complete except the dam closing off the Eastern Scheldt from the sea. In view of growing opposition to a complete closure, plans were revised in 1976, and instead of the dam, a storm surge barrier will be constructed. This barrier will reduce the tidal range in the Eastern Scheldt and will be closed during storm surges.

In support of engineering and environmental studies related to the construction and operation of this barrier, a large numerical model has been developed, which covers the Eastern and Western Scheldt and the adjacent offshore area. The section of the North Sea which is included in the model is about 120 km long and 30 km wide, running from Blankenberghe in Belgium to Scheveningen in the Netherlands (Fig. 1).

The bathymetry of the model area varies widely. In general it slopes from the shore to about 25 m at 30 km from the coast. In certain sections of the offshore area, the bottom is relatively flat; in other areas it has offshore bars and the bottom contains underwater sand dunes with a height of several meters. In the estuaries the tidal flow has scoured deep channels. The tidal flats near the North Sea are generally sandy, but the ecologically important tidal marshes located more inland contain much finer material.

The flow and the water levels in the region which is modeled are generally tide-induced. However, the influence of meteorological effects is always present and sometimes dominates water movements and water levels (storm surges). The influence of the fresh water discharges is of much less importance; generally their effects can only be noticed in the immediate vicinity of the discharge.

The tides in the offshore area of the model are part of the complicated tide system in the North Sea. The semidiurnal tidal wave propagates along the coast in a northeasterly direction. During this propagation the amplitude reduces from about 1.90 m near Blankenberghe to about .85 m near Scheveningen.

---

[1] Delft Hydraulics Laboratory, The Netherlands
[2] Rijkswaterstaat, Delta Service, The Netherlands
[3] The Rand Corporation, Santa Monica, California, U.S.A.

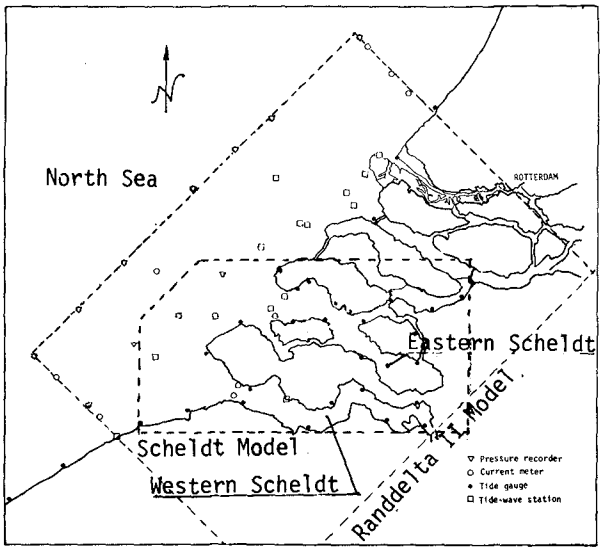

Fig. 1--Layout of models and location of recording stations

In the Eastern and Western Scheldt, the semidiurnal tidal wave penetrates into the estuary and is partially reflected. In the Eastern Scheldt the amplitude increases from 1.35 m near the mouth to 1.95 m at the eastern extremity; in the Western Scheldt the amplification is from about 1.75 m near Vlissingen to 2.30 m at the Dutch-Belgian border.

As the tides are waves, the best visual representation can be obtained by looking at amplitude and phase relations between stations. In Fig. 2 the results of such an analysis are presented in the form of a polar plot of frequency response estimates for the semidiurnal tide. The top part of the figure shows how the respective amplitude and phase relations were established by cross-spectral analysis and the locations of the recording instruments. All stations are numbered and the respective amplitude and phase are shown in relation to a station in the center of the model. For example, station 26 (Rak Zuid Volkerak) lags 1.6 hours behind the reference station 13 (BG II) and is about 1.6 times as large.

The diurnal tide is much smaller and is not much amplified in the model area. In some parts of the model area, the nonlinearities in the hydrodynamics generates strong overtides. This is particularly the case in the northern part of the model. Figure 3 shows the observed water levels obtained by a bottom pressure recorder during the survey described in Ref. 1, corrected for density variations, settling and atmospheric pressure. In the same graph, the quarter-diurnal tide component is shown. This component was obtained by filtering the tide data with Coulomy's quarter-diurnal bandpass filter, described by Godin [2]. The existence of these strong nonlinearities in the system complicated the modeling work considerably.

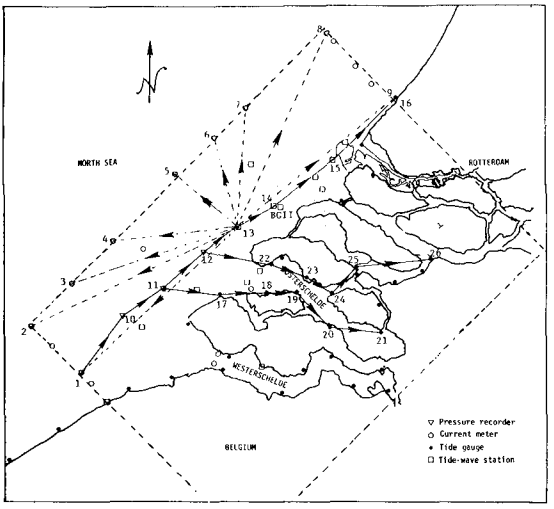

REF B.G. II
1 SCHEUR I
2 KNIKPUNT I
3 NOORD THORTONBANK
4 KNIKPUNT II
5 KNIKPUNT III
6 EURO 1A
7 KNIKPUNT IV
8 KNIKPUNT V
9 SCHEVENINGEN

SCHEUR I
10 OEURLOO
11 KALOO NOORD
12 MIDDENBANJAARO
13 B.G. II
14 B.G. V
15 M.A. III
16 SCHEVENINGEN

KALOO NOORD
17 OOSTKAPELLE
18 VLIETEPOLDER
19 COLIJNSPLAAT
20 HEMELDINGE
21 RAZERNIJPOLDER

MIDDENBANJAARO
22 BURGHSLUIS
23 ZIERIDZEE
24 STAVENISSE
25 KRAMMER
26 RAK ZUID VOLKERAK

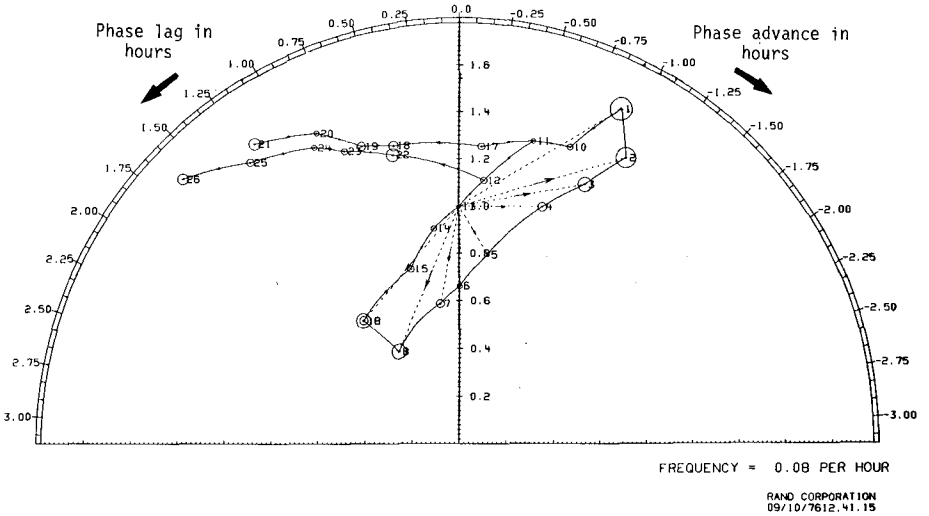

Fig. 2--Polar plot of the frequency response estimates of the semidiurnal tide from a central station (BG II) to other stations in the model area

The velocities in the model area vary considerably in space and time. The large variations which are present near tidal channels put high demands on the stability of the computation method and the accuracy of the representation of these spatial variations.

In the estuaries the tidal current can be as high as 1.50 m/s in the offshore area; the currents range from 0 to 1 m/sec.

The seaward boundaries of the Randdelta II model are situated at the same location as the boundaries of an earlier model with a much coarser grid. Only the model area at the northern end was reduced. The location of the boundaries of that model were determined on the basis of a numerical model study of the southern North Sea with a model described in Ref. 3. Studies with that model indicated that the influence of the closure dams in the Delta region on the water levels at the boundary of the Randdelta models would be very small--much smaller than the accuracy at which water level data can be obtained at that water depth. In part the exact location of the long open boundary was determined from the feasibility of data collection. As described in Ref. 1, many limitations existed in placing instruments in these heavily traveled waters.

At the boundary, water level and current data was measured, by which the boundary conditions for the model were well determined.

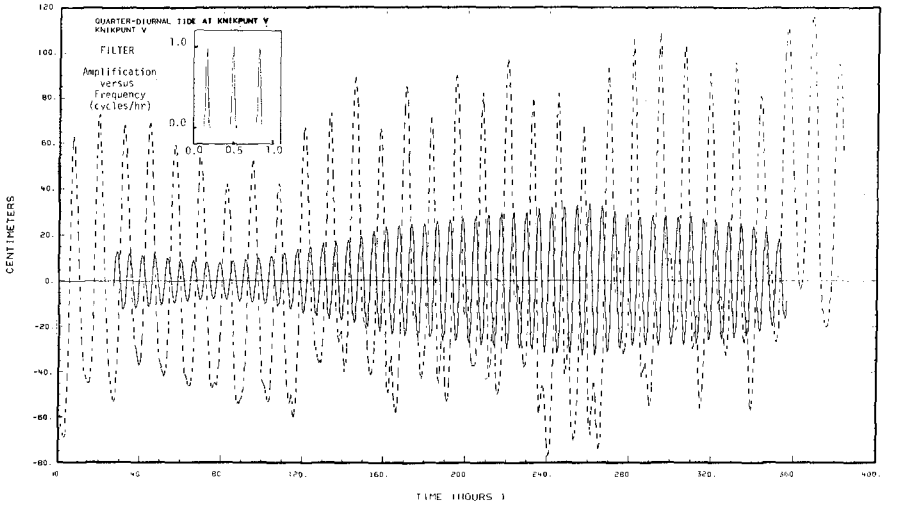

Fig. 3--Observed tides at a station in the corner of the model (Knikpunt V), together with the quarter-diurnal tide obtained from the record by a bandpass filter

II. MODEL FORMULATION

The model is based upon the so-called vertically integrated semi-momentum equations which have been derived in Ref. 4. In this case the atmospheric pressure differences are added as driving forces. The momentum equations now contain a viscosity term and pressure differences due to salinity gradients. The equations are written as

$$\frac{\partial U}{\partial t} + U\frac{\partial U}{\partial x} + V\frac{\partial U}{\partial y} - fV + g\frac{\partial \zeta}{\partial x} + \tfrac{1}{2}g\frac{H}{\rho}\frac{\partial \rho}{\partial x} + g\frac{U(U^2+V^2)^{\frac{1}{2}}}{C^2H} - \frac{\theta\rho_a W^2 \sin\psi}{\rho H} - \frac{\partial \wp}{\partial x} - k\left(\frac{\partial^2 U}{\partial x^2} + \frac{\partial^2 U}{\partial y^2}\right) = 0 \qquad (1)$$

$$\frac{\partial V}{\partial t} + U\frac{\partial V}{\partial x} + V\frac{\partial V}{\partial y} + fU + g\frac{\partial \zeta}{\partial y} + \tfrac{1}{2}g\frac{H}{\rho}\frac{\partial \rho}{\partial y} + g\frac{V(U^2+V^2)^{\frac{1}{2}}}{C^2H} - \frac{\theta\rho_a W^2 \cos\psi}{\rho H} - \frac{\partial \wp}{\partial y} - k\left(\frac{\partial^2 V}{\partial x^2} + \frac{\partial^2 V}{\partial y^2}\right) = 0 \qquad (2)$$

$$\frac{\partial \zeta}{\partial t} + \frac{\partial (HU)}{\partial x} + \frac{\partial (HV)}{\partial y} = 0 \qquad (3)$$

$$\frac{\partial (HP)}{\partial t} + \frac{\partial (HuP)}{\partial x} + \frac{\partial (HVP)}{\partial y} - \frac{\partial\left(HD_x \frac{\partial P}{\partial x}\right)}{\partial x} - \frac{\partial\left(HD_y \frac{\partial P}{\partial y}\right)}{\partial y} - R = 0 \qquad (4)$$

where D_x, D_y = dispersion coefficients
f = Coriolis parameter
g = acceleration of gravity
h = distance from the bottom to the reference plane
H = temporal depth ($= h + \zeta$)
k = horizontal velocity diffusion coefficient
P = vector of dissolved constituent concentrations
$\wp$ = atmospheric pressure
U = vertically averaged velocity component in x direction
V = vertically averaged velocity component in y direction
W = wind speed
ζ = water level elevation relative to a horizontal reference plane
θ = wind stress coefficient
ρ = density of water
ρ_a = density of air
ψ = angle between wind direction and the positive y direction

Several coefficients can be computed. The Chezy value can be computed from the Manning's coefficients and the temporal depth, and the dispersion coefficient from the temporal depth, the local velocity and the Chezy coefficient.

In the model a horizontal velocity diffusion can be used. From a theoretical point of view, the horizontal momentum diffusion is small, but because of computational effects, it may be desirable to use a value which is larger than we would expect from theory. More sophisticated users of the model would like to see a larger coefficient used only when considerable variations occur in the velocity field, for example, in such areas where we would expect vortex streets which we naturally cannot represent on a grid system. To accommodate such users we have introduced

$$k = k_o + k' |\partial_y \omega| (\Delta s)^2 \tag{5}$$

where $\omega = \frac{\partial U}{\partial y} - \frac{\partial V}{\partial x}$

The horizontal density gradient is computed from the salinity distributions and an equation of state. For the equation of state we use

$$\rho = (5890 + 38T - .375T^2 + 3S)/[(1779.5 + 11.25T - .0745T^2) - (3.8 + 0.01T)S + 0.698(5890 + 38T - 0.375T^2 + 3S)] \tag{6}$$

where T = temperature
S = salinity

The temperature differences in the model area appear to be small; also, the influence of temperature on density is small. Consequently, it can be assumed for the computation of density that the temperature is constant in the whole model area.

III. COMPUTATION APPROXIMATIONS

The model is based upon finite difference approximations of the partial difference equations (1)-(4). The grid system and the method of computation are an extension of an earlier computation method described in Ref. 4. To write these finite difference equations, the following notations for averages, derivatives and time shifts are used:

$$\overline{F}^x = \tfrac{1}{2}\left\{F[(j+\tfrac{1}{2})\Delta x, k\Delta y, n\Delta t] + F[(j-\tfrac{1}{2})\Delta x, k\Delta y, n\Delta t]\right\} \tag{7}$$

$$\delta_x F = \frac{1}{\Delta x}\left\{F[(j+\tfrac{1}{2})\Delta x, k\Delta y, n\Delta t] - F[(j-\tfrac{1}{2})\Delta x, k\Delta y, n\Delta t]\right\} \tag{8}$$

$$\nabla^2 F = \frac{1}{(\Delta x)^2}\left\{F[(j+1)\Delta x, k\Delta y, n\Delta t] - 2F[j\Delta x, k\Delta y, n\Delta t] + F[(j-1)\Delta x, k\Delta y, n\Delta t] + F[j\Delta x, (k+1)\Delta y, n\Delta t] - 2F[j\Delta x, k\Delta y, n\Delta t] + F[j\Delta x, (k-1)\Delta y, n\Delta t]\right\} \tag{9}$$

$$F_+ = F[j\Delta x, k\Delta y, (n+\tfrac{1}{2})\Delta t] \tag{10}$$

$$F_{-} = F[j\Delta x, k\Delta y, (n-\tfrac{1}{2})\Delta t] \tag{11}$$

$$\delta_{+\frac{1}{2}t}F = \frac{2}{\Delta t}\left\{F_{+} - F\right\} = \frac{2}{\Delta t}\left\{F[j\Delta x, k\Delta y, (n+\tfrac{1}{2})\Delta t] - F(j\Delta x, k\Delta y, n\Delta t)\right\} \tag{12}$$

In the finite difference equations variables which are computed by iterations are indicated by special symbols, for example, F_{*}, $F_{\dagger}$.

By the introduction of iterations in determining the value of certain variables, the user of the model has some choice in the approximations of the partial differential equations. This choice refers mainly to the time level at which the approximation of a certain term is made, thus we can say that the user has certain integration options.

The integrations are performed with two different operations. In one of the operations we are computing the new velocity components and the new water levels at timestep $n+\frac{1}{2}$ from information which is available at timestep n and timestep $n-\frac{1}{2}$ by use of

$$\delta_t u - \bar{\bar{f}}^{xy}\bar{v}^{xy} + 1/3\left\{\left(\overline{\overline{u_{*}}^{x}u_{*}}^{x}\right)_x + \tfrac{1}{2}\overline{\left[u_{*}(u_{*} + \Delta^2\nabla^2 u_{*})\right]^{x}}_{x} + 2\bar{\bar{v}}^{xy}\overline{(u_{*})_y}^{y} + \overline{\bar{v}^{x}(u_{*})_y}^{y}\right\}$$

$$+ g\overline{\delta_x\zeta}^{t} + \tfrac{1}{2}\frac{g}{\rho}(\bar{h}^{y} + \bar{\zeta}^{x})\,\delta_x\rho + g\,\frac{\bar{u}^{t}\left[(u_{*})^2 + (\bar{\bar{v}})^2\right]^{\frac{1}{2}}}{(\bar{h}^{y} + \bar{\zeta}^{x})(\bar{C}^{x})^2}$$

$$- \frac{\theta\rho_a W^2 \sin\psi}{\rho(\bar{h}^{y} + \bar{\zeta}^{x})} - \delta_x\wp - k\nabla^2 u_{-} = 0$$

$$\text{at } j+\tfrac{1}{2},\ k,\ n \tag{13}$$

$$\delta_{+\frac{1}{2}t}\zeta + \delta_x\left[(\bar{h}^{y} + \overline{\zeta_{+}}^{x})u_{+}\right] + \delta_y\left[(\bar{h}^{x} + \bar{\zeta}^{y})v\right] = 0$$

$$\text{at } j+\tfrac{1}{2},\ k,\ n \tag{14}$$

where $\Delta = \Delta x = \Delta y$

The integration can be made without iteration at which u_{*} and h_{+} are taken at the time level of the last available data, which would be $n-\frac{1}{2}$ for u and n for ζ. The results of this step can also be introduced again into u_{*} and ζ_{+}, for example, by using the average of the newly-found velocity and u_{-}. Many options are available to the investigator, as described in Ref. 5.

Generally initially an option is used which results in a second order approximation in time and space of all terms in the equations except the momentum diffusion term. For constituent i, the mass-balance equation is approximated in finite-difference form at time level n by

$$\delta_{+\frac{1}{2}t}\left[P_i(\overline{\overline{h}} + \zeta)\right] + \delta_x\left[(\overline{\overline{h}}^y + \overline{\zeta}^x_+)u_+\overline{P}^x_{i_+}\right] + \delta_y\left[(\overline{\overline{h}}^x + \overline{\zeta}^y)v\overline{P}^y_i\right]$$
$$- \delta_x\left[(\overline{\overline{h}}^y + \overline{\zeta}^x_+)D_{x_+}\delta_x P_{i_+}\right] - \delta_y\left[(\overline{\overline{h}}^x + \overline{\zeta}^y)D_y\delta_y P_i\right]$$

$$+ \sum_{\ell=1}^{i-1}(\overline{\overline{h}} + \zeta_+)K_{i\ell}P_{\ell_+}\alpha_i + \overline{(\overline{\overline{h}} + \zeta)K_{ii}P_i}^{t/2} + \sum_{\ell=i+1}^{\ell_{max}}(\overline{\overline{h}} + \zeta)K_{i\ell}P_\ell\beta_i$$

$$+ (\overline{\overline{h}} + \zeta)S_i = 0 \qquad \text{at } j, k, n \tag{15}$$

where $\alpha_i = \begin{cases} 0 & i = 1 \\ 1 & 1 < i \le \ell_{max} \end{cases}$

$\beta_i = \begin{cases} 0 & i = \ell_{max} \\ 1 & 1 \le i < \ell_{max} \end{cases}$

ℓ_{max} = maximum number of constituents

K = reaction matrix term

No iteration is required for the computation of the concentrations.

In the second operation, the new velocity component v and the new water levels at timestep n+1 are computed from information which is available at timestep n+½ and timestep n by use of

$$\delta_t v + \overline{\overline{fu}} + 1/3\left\{2\overline{\overline{u(v_*)_x}}^x + \overline{u^y(v_*)_x}^x + \overline{(v_*^y v_*^y)_y} + \tfrac{1}{2}\overline{\left[v_*(v_* + \Delta^2\nabla v_*)_y\right]}^y\right\}$$
$$+ g\overline{\delta_y\zeta}^t + \tfrac{1}{2}\frac{g}{\rho}(\overline{\overline{h}}^x + \overline{\zeta}^y)\,\delta_y\rho + g\frac{\overline{v}^t[(\overline{\overline{u}})^2 + (v_*)^2]^{\frac{1}{2}}}{(\overline{\overline{h}}^x + \overline{\zeta}^y)(\overline{C}^y)^2}$$
$$- \frac{\theta\rho_a W^2\cos\psi}{\rho(\overline{\overline{h}}^x + \overline{\zeta}^y)} - \delta_x\rho - k\nabla^2 v_- = 0$$
$$\text{at } j, k+\tfrac{1}{2}, n+\tfrac{1}{2} \tag{16}$$

$$\delta_{+\frac{1}{2}t}\zeta + \delta_x\left[(\overline{\overline{h}}^y + \overline{\zeta}^x)u\right] + \delta_y\left[(\overline{\overline{h}}^x + \overline{\zeta}^y_+)v_+\right] = 0$$
$$\text{at } j, k+\tfrac{1}{2}, n+\tfrac{1}{2} \tag{17}$$

It will be noted that u is computed only in the half-integer timesteps,

while v is computed in the integer value of the timestep, and the water levels are computed every half timestep.

The concentrations are also computed every half timestep, and in the second operation of the computation method the following equation is used:

$$\delta_{+\frac{1}{2}t}\left[P_i(\overline{\overline{h}} + \zeta)\right] + \delta_x\left[(\overline{h}^y + \overline{\zeta}^x)u\overline{P}^x_i\right] + \delta_y\left[(\overline{h}^x + \overline{\zeta}^y_+)v_+\overline{P}^y_{i_+}\right]$$

$$- \delta_x\left[(\overline{h}^y + \overline{\zeta}^x)D_x\delta_x P_i\right] - \delta_y\left[(\overline{h}^x + \overline{\zeta}^y_+)D_{y_+}\delta_y P_{i_+}\right]$$

$$+ \sum_{\ell=1}^{i-1}(\overline{\overline{h}} + \zeta)K_{i\ell}P_\ell\alpha_i + \overline{\overline{(\overline{\overline{h}} + \zeta)K_{ii}P_i}}^{t/2} + \sum_{\ell=i+1}^{\ell_{max}}(\overline{\overline{h}} + \zeta_+)K_{i\ell}P_{\ell_+}\beta_i$$

$$+ (\overline{\overline{h}} + \zeta)S_i = 0 \qquad \text{at } j, k, n+\tfrac{1}{2} \tag{18}$$

The rather extensive fourth order expressions for the advection terms of the momentum equations are required for stability. In the large computational fields with much variation in velocities, simple second order approximation of the advection terms appeared to be unstable, generating interactions between the two momentum equations, and thus generating high vorticities with the dimension of the grid spacing. The Arakawa [6] expression used here prevents this occurrence.

The model requires a large number of time-varying boundaries. At the seaward boundaries, water levels (or currents) are prescribed by linear interpolation of amplitudes and phases between points of prototype measurement, as described in Ref. 1.

If water levels are used as boundary conditions, the advection terms near the seaward boundaries of the model are omitted. This omission simplifies the boundary description. It can be shown that, in addition to the water levels, velocity data is required to describe the boundary when the flow is into the model when the advection terms are included. The contributions of these terms are very small, as the velocities in the Randdelta II model are either nearly perpendicular or nearly parallel to the boundary and the rate of change is also small. More important than the advection terms are the contributions of the pressures induced by salinity differences. The salinities are prescribed during inflow and computed from inside the field during outflow. The transition in the salinity between outflow and inflow is according to half the cycle of a cosine function over a period which can be set.

All discharges into the system, wind intensity and direction and atmospheric pressures are time-varying.

The computations of the tidal marshes and flats are described in Ref. 5.

IV. MODELING SYSTEM

For successful model investigations with numerical models a system of interlocking programs is required for data handling, simulation and graphical representation. The system used in this investigation has three major parts, namely, the Input Data Processor (IDP), the Simulation program (SIMSYS2D) and the Simulation Data Display system (SDD).

One of the functions of IDP is to order the input data from a logical input form into a form that permits it to be readily used by the simulation. For example, discharges and wind speed and direction can be inserted as individual time series. The processor will order all this data in a sequence fit for simulation. Another very important function of this processor is to document the data in an easily readable report and in easily accessible data files for graphical representation.

The system which is used for data display is designed to make charts and graphs of simulation results and inputs for study and reporting purposes. For example, Fig. 4 shows a chart made with the system to indicate which area is under water when the static water level is .50 m above the reference level. Also, comparisons of simulation results with other simulation data or with observed data can be made.

The system is designed to be used by civil engineers. Its operation requires no special knowledge of the computer science aspects of data handling and manipulation other than a thorough understanding of the computation procedures outlined briefly in the previous section of this paper.

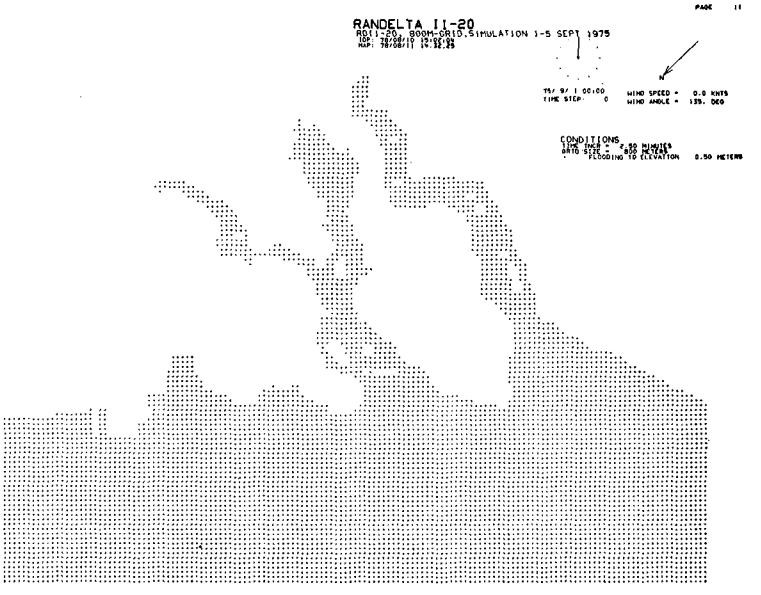

Fig. 4--SDD chart of submerged area at a still water level of 0.5 m above the reference level

V. ASPECTS OF TIDAL WAVE PROPAGATION IN THE MODEL AREA

The tidal flow in the sea area of the Randdelta II model is part of the flow in a much larger system, thus to properly represent this flow in the model area, boundary conditions along the open sides of the model have to be obtained. These boundary conditions can be derived from a model covering a larger area or from a field survey. For some of the studies with the model involving storm surges, results from a larger modcl are being used, but for the adjustment of the model, results of a large field survey are available in which water levels and currents on each of the open sides of the model were determined. In the computational procedures of the simulation system water levels or currents could be used as boundaries. Consequently, in the beginning of the investigation the question arose as to what would be the best combination of water level and current boundary conditions, taking into account that the boundary data contain errors and that these errors may be amplified. For example, if only flow is used on all boundaries, their errors would lead to a gradual increase or decrease of the water levels in the system. Naturally, it would be better if at least one of the boundaries was prescribed by water levels.

The type of boundary conditions along the seaward sides of the model should be chosen in such a manner that

- errors in the boundaries have a direct and easily detectable response in water levels and currents of the model results.
- errors in the boundary are not amplified in the interior of the model.
- errors in amplitudes should only influence the amplitudes in the system and errors in phase should only influence the phases of the tide.
- the vertical tide in the sea area just outside the estuary is not much influenced by the choice of the Manning's coefficient and the accuracy of the bathymetry.

If the last condition can be fulfilled, the estuaries can be adjusted more or less independent from the adjustment of the offshore area of the model.

The three open boundaries of the model indicated in Fig. 5 are each in a different position as to the semidiurnal tidal wave, which is the dominating wave in the system. The tidal wave enters the model through boundary (1) and exits through (3). Boundary (2) is nearly parallel to the direction of tidal wave propagation. For each of these three boundaries we have two choices, namely, a water level boundary, designated by H in the following discussion, and a flow boundary, designated by Q.

Table 1 shows the possible combinations of boundary conditions. Note that the combinations a through d are the same as the combinations e through h, except in the condition for boundary (2).

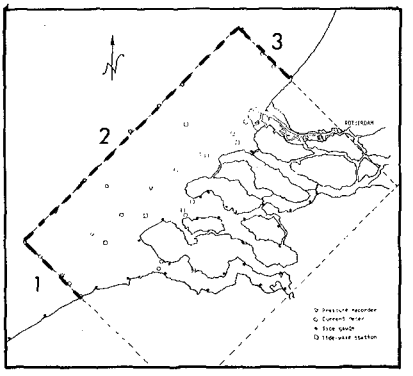

Fig. 5--Boundary designation

Table 1

Combination	Boundary 1	2	3
a	H	H	H
b	Q	H	Q
c	Q	H	H
d	H	H	Q
e	H	Q	H
f	Q	Q	Q
g	Q	Q	H
h	H	Q	Q

The following suppositions can be made:

- The errors are relatively small compared to the measured values.
- The errors are more or less equally distributed along the boundary.
- Those errors are gradually diminishing along the perpendicular boundary 2.

These suppositions are partially supported by the fact that in preparing the results of the survey efforts were made to make the results coherent. In section I it is noted that the tide progresses parallel to the coast. This and the aforementioned suppositions make it plausible to first investigate the interaction of boundaries 1 and 3 in a one-dimensional analytic model with the axes along boundary 2, thus leaving the possibility of considerably reducing the number of combinations to be investigated later in connection with boundary 2.

For the one-dimensional analytic model the area in view was schematized to a channel with a constant width and depth. To find an analytic solution to the partial differential equations describing the long-wave motion in a tide, the equations are linearized with respect to the roughness term. Furthermore, the advection term and the Reynolds stresses in the momentum equation and the wave height with respect to the depth are neglected.

The following partial differential equations remain:

$$\frac{\partial Q}{\partial t} + \lambda Q + gDB \frac{\partial \zeta}{\partial x} = 0 \tag{19}$$

$$B \frac{\partial \zeta}{\partial t} + \frac{\partial Q}{\partial x} = 0 \tag{20}$$

where B = width (m)
D = depth (m)
g = gravity acceleration (m/s^2)
Q = flow (m^3/s)
ζ = wave height (m)
λ = roughness parameter (1/s), equal to $\frac{gu}{C^2 D}$, with
C = Chezy parameter ($m^{\frac{1}{2}}/s$)
u = representative velocity (m/s)

These equations have a general solution of the type:

$$Q(x,t) = A_Q(X) \cos [\omega t + P_Q(X)] \tag{21}$$

$$\zeta(x,t) = A_\zeta(X) \cos [\omega t + P_\zeta(X)] \tag{22}$$

By substituting Eqs. (21) and (22) into Eqs. (19) and (20) and by use of boundary conditions, solutions for the amplitudes and phases of the tidal waves can be obtained. As the system is linear, several constituents can be considered, but in the analysis only the semidiurnal tide was considered.

From the field survey, good estimates of water levels and currents of the semidiurnal tide could be made. These were used for the combinations a through d of Table 1. For the depth the average of the region was taken and the friction factor was estimated. In these tests comparisons were made of the horizontal and vertical tide for each combination with increased and decreased amplitudes at one of the boundaries and with phase shifts at that boundary. Also, tests were made with increased and decreased depth and bottom friction. Some of the combinations of boundary conditions were very sensitive to changes in the friction factor. For example, if an H boundary is taken at (1) and a Q boundary at (3), a decrease in the resistance factor of 20% increases the amplitude at boundary (3) by about 50%. The distribution of the error along the model is shown in Fig. 6 for an increase and decrease of the friction factor of 20%. Figure 7 shows the distribution of the error in a similar manner for Q.

The result of this analysis was that water levels at each of the sides of the model was by far the best combination. In that combination the model is insensitive in the water levels to changes in bottom friction and has a relatively small response in the amplitude and phase of the horizontal tide to changes in bottom friction.

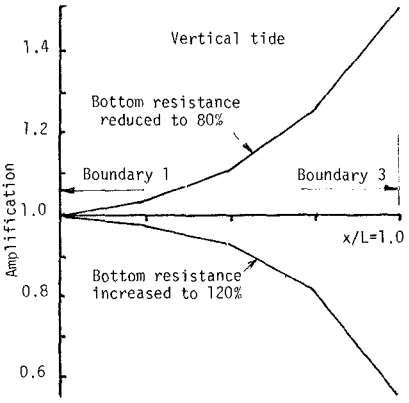

Fig. 6--Influence of change in bottom resistance factor λ on the vertical tide by use of H at boundary 1 and Q at boundary 3

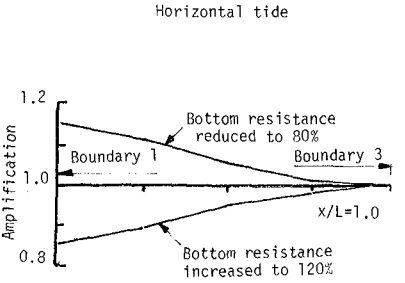

Fig. 7--Influence of change in bottom resistance factor λ on the horizontal tide by use of H at boundary 1 and Q at boundary 3

After having established the best combination of boundary conditions for boundaries 1 and 3, an analysis was made of the long open boundary 2. This analysis was made with a submodel of the Randdelta II model. This submodel, described in section VI, models the offshore area of the Randdelta II model with a grid size of 1600 m. Simulations with flow data obtained from the field survey at boundary 2 indicated that errors in Q had a large effect upon the water levels in the model region. Errors in water levels along boundary 2 appear to have a minimal effect upon water levels in the model area and would affect only the flow field locally. Consequently, a water level boundary condition was also chosen here. The errors in that water level boundary were reduced by procedures outlined in Ref. 1.

The results of the analysis of the boundary conditions for this offshore area are not generally applicable. The optimum choice depends on the size of the offshore area to be modeled, the depth and the bottom friction.

For example, an extensive research effort with one- and two-dimensional models made by the Delft Hydraulic Laboratory, for determining the optimal combination of boundaries for a hydraulic model of an offshore area near the entrance of the New Waterway, indicated that a combination of H and Q boundaries was to be preferred. This model covers a small section of the Randdelta II model.

To assist in the adjustment of the estuary sections of the Randdelta II model, a one-dimensional analysis of the tidal wave propagation into the Eastern and Western Scheldt was also made. As shown in Figs. 8 and 9, incremental increases in depth and the linear bottom resistance term do not give a linear change in amplification and phase shift.

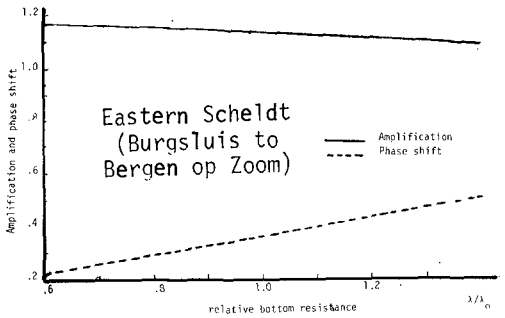

Fig. 8--Influence of change in bottom resistance on amplification and phase lag for the Eastern Scheldt

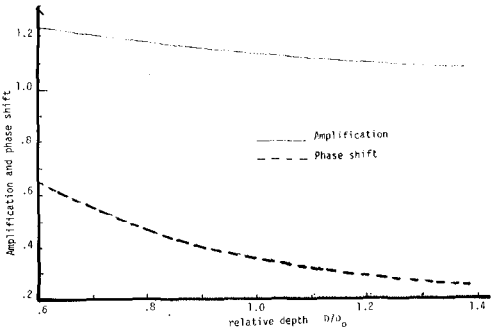

Fig. 9--Influence of change in depth on amplification and phase lag for the Eastern Scheldt

VI. SUBMODELS

The adjustment of tides and currents in the estuaries appeared to be difficult. The estuaries are relatively poorly represented on the 800m grid, certainly in comparison with the offshore area. To progress more rapidly with the adjustments of these sections of the model, several submodels were built based upon data abstracted from the Randdelta II model.

The depth array for the Randdelta II model was obtained by drawing all cross-sections at lines through the depth grid points which are more or less perpendicular to the main current direction. Subsequently depth approximations at the grid points were made in such a manner that the area of the cross-section in the model is about the same as in nature. Care was taken that channels were well represented. With the submodels the opportunity existed to verify the adequacy of this representation.

The first step in the adjustment process is to check the submergence of tidal flats. The criteria used in the flow simulation are quite complicated, mainly due to the demands of conservation of the mass of water and the mass of the constituents.

The submergence is checked by procedures in the SDD system which operate in the same way as in the simulation (Fig. 4). With the SDD system charts can then be made indicating the area which is submerged at certain specified water levels. On these charts it can be checked if small channels become closed by the procedures.

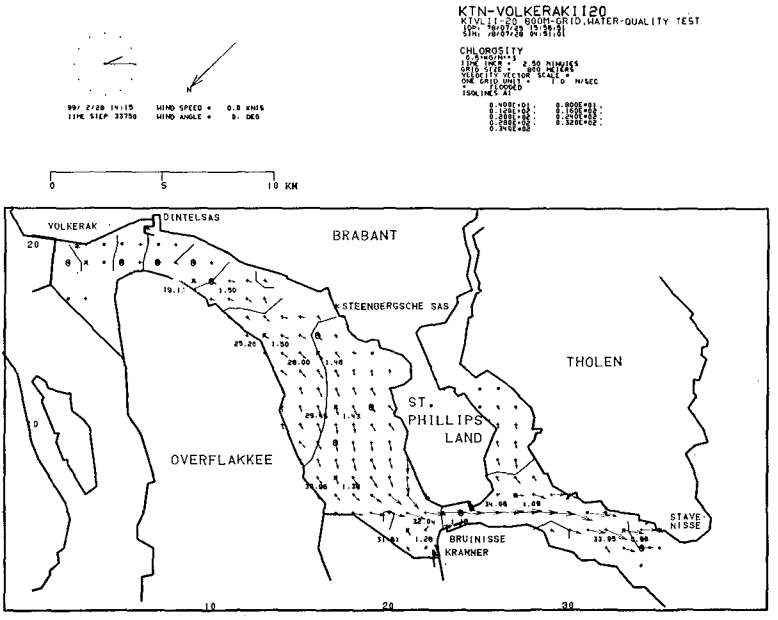

Fig. 10--Chlorosity distributions computed with the KTN-Volkerak II submodel of the Randdelta II model

Figure 10 shows a typical graphical result obtained from a simulation with a submodel. For the adjustment of this submodel observed water levels were used as boundary conditions. The first simulation with this submodel was made with an initial estimate of the Manning's coefficient. Subsequently a simulation was made in which in a certain well-defined region between two water level stations the Manning's coefficient was increased. Also a simulation was made in which the depth in that defined region was increased proportionally 10%, but using Chezy values in that region obtained from the original run of that region. By analyzing the computation results for water levels, functional relationships between changes in Manning's coefficient and depth increases for the amplification and phase lag of the semidiurnal tide in the considered section of the model could be determined. From these relations it was possible to make a good estimate of the required changes to match the propagation in the model with that in the prototype. If depth changes were required, those were made by reviewing the used depth approximation in relation to the actual cross-sections. Other sections of the submodel were adjusted in a similar fashion.

The depth appeared to be rather sensitive in the shallow water areas and the shape of the tidal curve in the eastern part of this submodel is determined to a very large extent by the time of submergence of the tidal marshes. Even though it was realized that only a rough approximation of the flow in this submodel could be obtained, considerable

effort was expended, as the phase of the currents at the boundary of the submodel would be of importance in simulating the Eastern Scheldt proper. In this submodel, fresh water discharges through sluices at the eastern extremity of the model were present. These discharges are of considerable magnitude, and in a part of the submodel area salinity differences in the vertical existed in the simulation period. Consequently, the basic model assumption that the area is well mixed was violated. The salinity differences in the vertical induce vertical circulations which can be represented locally by a larger diffusion coefficient.

To adjust this coefficient long duration simulations were made of a condition in which the discharge into the system was kept approximately constant. The model was started with the salinity of the open boundary everywhere in the whole model. By simulating two months and adjusting the diffusion coefficient in the region with vertical density differences, equilibrium conditions could be obtained which matched quite well the observed conditions.

Dronkers [7] presents an analytical study of the longitudinal dispersion in shallow well mixed estuaries based upon a study of exchange processes in the model area. He concluded that for well mixed systems, in addition to the dispersion process in the main channel, the exchange of water between the channel and the tidal flat or marsh area is of importance, as well as the mixing process on the tidal flat itself. As the water movements and the resultant exchanges are apparently quite well represented even with the relatively coarse grid, no further adjustment of diffusion coefficients in the well mixed region of the model other than the original estimate was required.

This submodel was also used in many experiments for checking and evaluating computation procedures. It was found that the computation is insensitive to the time levels in the advection terms, and that the phase of the tide is influenced when the time step is increased beyond 2.5 minutes.

In addition to the submodels which have the same grid size and depth as the Randdelta II model, a model of the offshore area with a grid size of 1600m was used in the adjustment process. This model had the same seaward boundaries as the Randdelta II model, and it had water level boundaries at the mouths of the Eastern Scheldt and Western Scheldt.

This model was relatively small and inexpensive to run. Many effects in this offshore zone could be studied effectively with this model. For example, the boundary conditions developed by cross-spectral analysis, as described in Ref. 1, were tested and evaluated with this model. Presently it is being used to evaluate the seaward boundaries for storm surge conditions, which were abstracted from a model of a section of the North Sea.

The Randdelta II model will furnish the boundary conditions of a model of the Eastern and Western Scheldt and a small adjacent offshore area with a 400m grid (Fig. 1). This model will be used for more detailed computations. Since this model is very large, submodels are again being used for adjustment and for experiments.

VII. MODEL ADJUSTMENT AND VERIFICATION

Modeling with a numerical model requires large data sets, and setting up the Randdelta II model has been a major effort. Much of the time-varying data for the tidal inputs originated from a field survey (Ref. 1), but also much data from other sources were used.

For example, all the major discharges in the system had to be obtained from the different logs which were kept by government officials at many places. Weather data had to be obtained and digitized. As already mentioned, determining the depth array from various survey charts was a major undertaking, and all data for making charts used for graphical representation of water level, velocity and concentration fields had to be digitized. Furthermore, all coordinates of the measuring stations on the national grid system had to be translated to those on the computational grid so that the closest available grid point can be used for abstracting similar data out of the model.

After the adjustment of the submodels, the depth and Manning's data were transferred back into the Randdelta II model and a series of experiments were made. The studies about the propagation of the semidiurnal tidal wave in the offshore area and in the estuaries gave guidance as to making increasingly better fits between observed and computed data. Even though the model is not considered completely adjusted in all respects, the agreement between observed and computed is good (Fig. 11). In one of the four graphs, the observed as well as the input tide is shown. All other graphs show the observed and computed vertical tides.

The recording station Steenbergse Sas is about 90 km from the closest open boundary and the recording station Baarland about 80 km. The small disturbances shown in the computed record for the station Steenbergse Sas originate from the incremental changes in the land-water boundary by the computation procedures.

The agreement between the observed magnitudes of currents and directions is also good, particularly if one takes into account that the observed currents are obtained at a certain point in a vertical. Figure 12 shows a comparison of currents. The Knikpunt III station is near the boundary and reflects all errors made in the data inserted.

With the simulation system, charts can be made of the velocity distributions at a particular time. Figure 13 shows such a velocity distribution on a much reduced scale. Note that extensive areas in the estuaries are exposed.

Presently, the model has been verified only to a limited extent by use of boundary data not previously used for adjustment. The results are very similar to those shown. Since it is the intention to use the model also for time periods at which no boundary input data are available, the verification process has to include the prediction of the boundaries from the fixed stations.

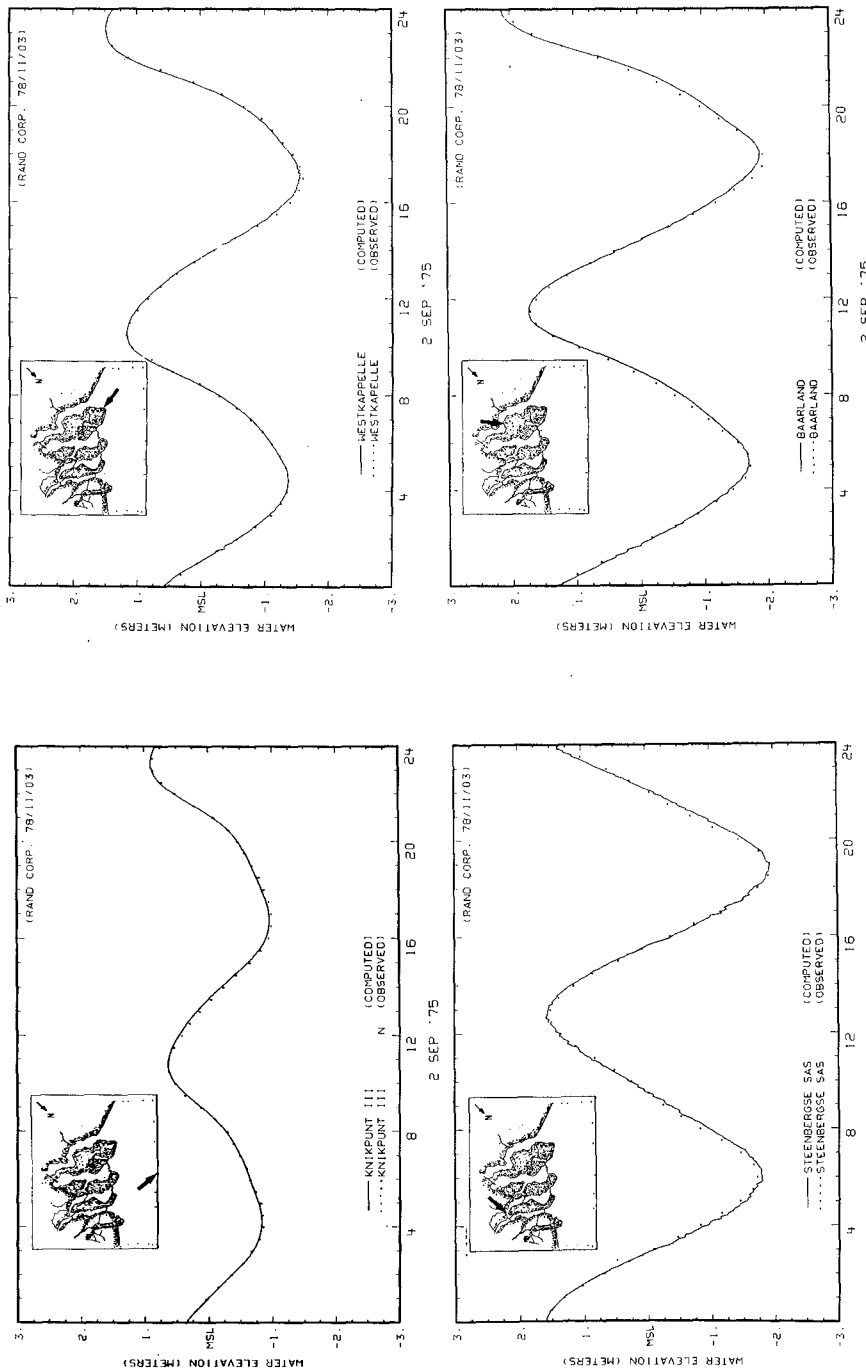

Fig. 11--Computed and observed water levels at four locations for September 2, 1975

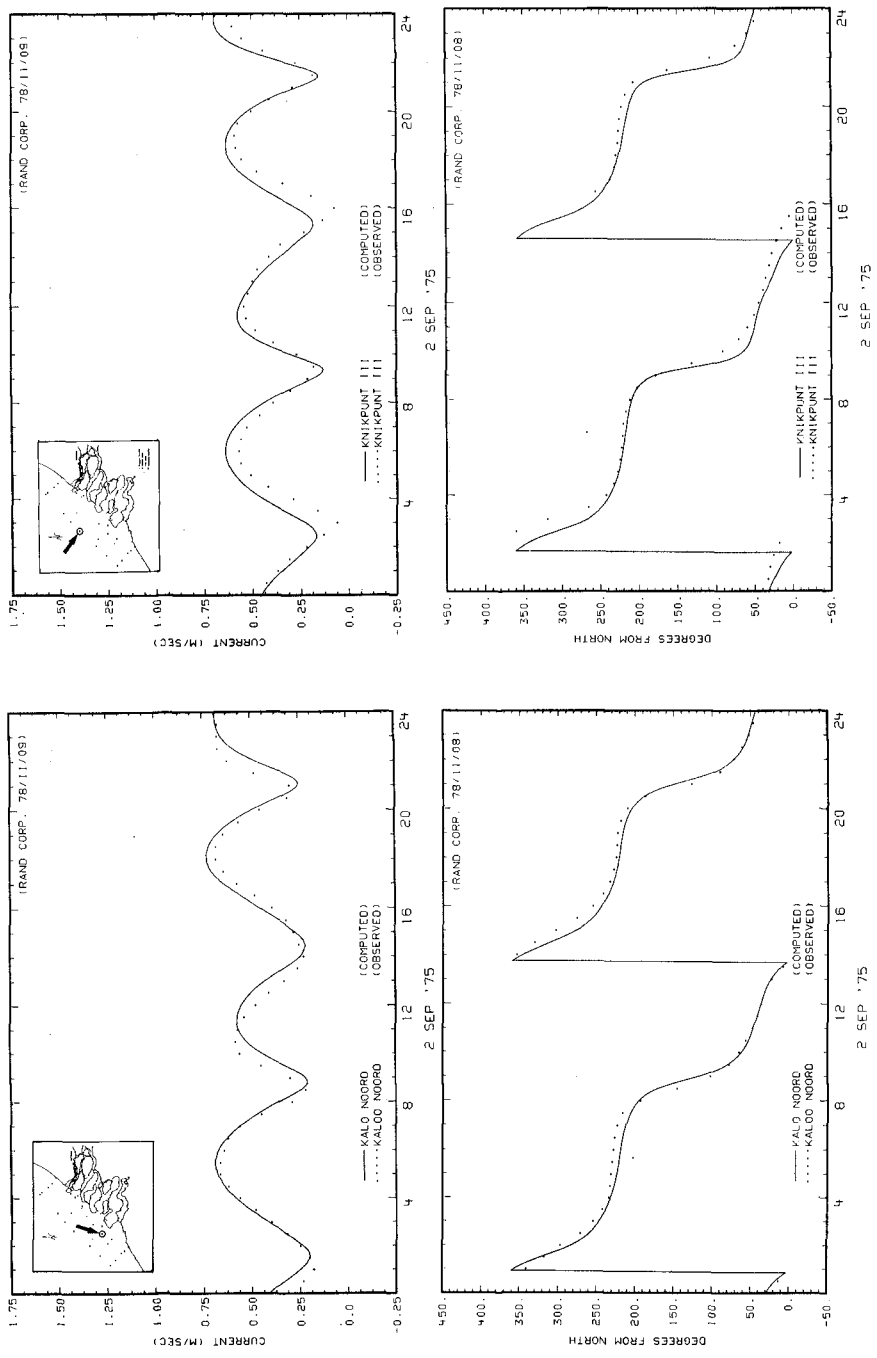

Fig. 12--Computed and observed current magnitudes and directions at two stations for September 2, 1975

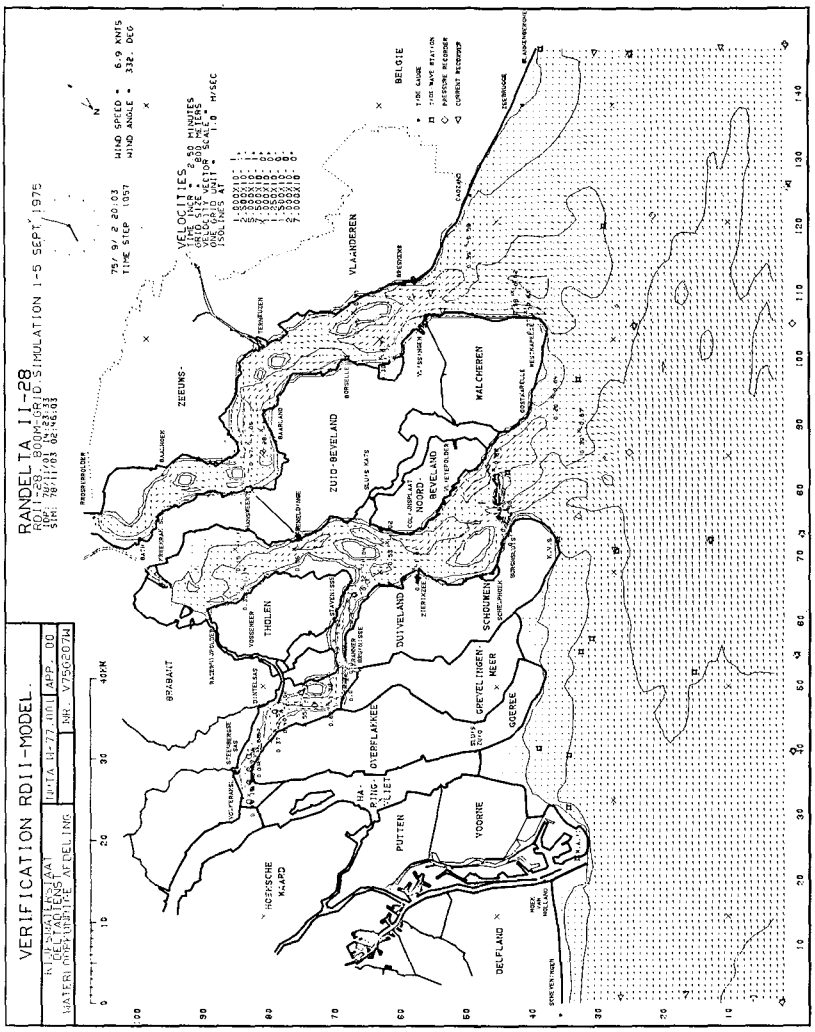

Fig. 13--Computed velocity distribution on September 2, 1975 at 20:03 hrs

REFERENCES

1. Van de Ree, W. J., J. Voogt and J. J. Leendertse, "A Tidal Survey for a Model of an Offshore Area," *Proc. 16th Int. Conference on Coastal Engineering*, 1978.

2. Godin, G., *The Analysis of Tides*, University of Toronto Press, Toronto, 1972.

3. Leendertse, J. J., *Aspects of a Computational Model for Long-Period Water-Wave Propagation*, The Rand Corporation, RM-5294-PR, May 1967.

4. Leendertse, J. J., and E. C. Gritton, *A Water Quality Simulation Model for Well-Mixed Estuaries and Coastal Seas: Vol. II, Computation Procedures*, The Rand Corporation, R-708-NYC, July 1971.

5. Leendertse, J. J., C. N. Johnson, and A. B. Nelson, *The SIMSYS/WAQUA System for Two-Dimensional Modeling of Estuaries and Coastal Seas*, The Rand Corporation, (to be published).

6. Grammeltvedt, A., "A Survey of Finite-Difference Schemes for the Primitive Equations for a Barotropic Fluid," *Monthly Weather Review*, Vol. 97, No. 5, May 1969.

7. Dronkers, J., "Longitudinal Dispersion in Shallow Well Mixed Estuaries, *Proc. 16th Int. Conference on Coastal Engineering*, 1978.